Supplementary figure 1.

A) Representative photographs of 40 WT, 30 TLR2 KO and 30 TLR9 KO mice with skin tumors (left) and 34 TLR4 and 30 MyD88 KO mice with or without papillomas (right). B) Hematoxylin-eosin stained invasive carcinoma (left) and papilloma (right) tumor samples from the above TLR2 and TLR4 KO mice, shown in the inset fig A. Histological analyses of equal sized papillomas in different groups were similar.

Supplementary figure 2.

Environmental TLR4 is not required for the growth of established carcinomas or tumor cell lines. A) Primary carcinomas from WT mice were cut into small pieces of 1 mm and subcutaneously transplanted into naive WT and TLR4 KO mice. Transplanted tumors in both groups of mice were growing in a similar manner over time (n=14 mice for each genotype). B) $5x10^5$ B16F10 melanoma cells were injected subcutaneously in WT and different TLR/MyD88 KO mice. Mice were followed for tumor growth. B16 melanoma growth was similar in all the groups except TLR2 KO that showed a significant delay in growth of melanoma compared to the other groups. Data represents means +/- standard deviation of the mean (n=10 for each genotype) and the results are representative of at least two independent experiments. * $P<0.05$, NS = not significant.

Supplementary figure 3.

A) Real-time PCR analysis for TNF-α expression in the skin at 12h, 24h, 48h, 1 week and 2 week (represented in days) after CO treatment is shown. B) TPA (10 mg) was applied topically on the shaved skin of WT or TLR4 KO mice and skin was collected after 12h for RNA analyses. Real-time PCR analysis for inflammatory cytokine expression in the skin after 12h of TPA treatment is shown. Results are expressed as fold induction over acetone-treated skins in each group after normalization to L32 mRNA. Values represent means +/- standard deviation of the mean from at least five mice in each group. The experiment was repeated

twice with similar results. * P<0.05, NS = not significant. C) Infiltration of CD11b positive cells (left) and granulocytes (Gr1, right) in the skin of WT and TLR4 KO mice treated with CO or acetone and analyzed by FACS at different time points. Values represent mouse skin samples from 3-5 mice and the experiment was repeated at least twice.

Supplementary figure 4.

Real-time PCR analysis for KC and MIP-2 expression in the skin at 6h, 12 h, 24h, 48h after CO treatment is shown. Results are expressed as fold induction over acetone-treated skins in each group after normalization to L32 mRNA. Values represent means +/- standard deviation of the mean from at least five mice in each group. * P<0.05

Supplementary figure 5.

Recruitment of inflammatory cells is dependent on TLR4 positive BM cells.

A) Immunofluorescence staining for Gr-1 (red) and dapi (blue) in the skin from chimeras taken 24h after CO (upper panel) or acetone (lower panel) treatment. Images are representative from three skins samples from each chimeras and the experiment was repeated twice. Scale bar = 250μm. B) Graph represents the quantification of Gr1 positive cells in at least three different slides/condition.

Supplementary figure 6.

A) Schematic representation of skin carcinogenesis protocol for mice treated with LPS and croton oil. 10μg of LPS per mouse was used either alone or in combination with croton oil for 34 weeks. B) Average number of papillomas per mouse in different mice group is shown over time. C) Percentage of tumor free mice over time is shown. N=15 for each group. One experiment was carried out. *, p<0.05, NS = not significant.

Supplementary figure 7.

A) Release of HMGB1 by ELISA in skin culture supernatants. The skins were removed at the indicated time points after single treatment with DMBA or croton oil and cultured in medium for 20h. Results are expressed as fold production over acetone-treated skins in each group. Values represent means +/- standard deviation of the mean from at least three mice from each group and the experiment was repeated twice. B) Graph represents percentage of live, apoptotic (Annexin V+) and necrotic/late apoptotic (Annexin V/PI double positive) cells based on the gated channels. Values represent means +/- standard deviation of the mean from at least three mice in each group. *, $p<0.05$ between CO or DMBA+CO groups versus control, Acetone (Ac) or DMBA groups.

Supplementary Fig. 8

$2X10^5$ BMDCs from WT and TLR4 KO mice were stimulated either directly with DMBA (1μM) or croton oil (0.5mg/ml), or indirectly with the supernatants (1:1) from keratinocytes treated or not with DMBA (1μM), or croton oil (0.5mg/ml). Supernatants were collected after 20h and analyzed for the release of TNF-$\propto$. The experiment was repeated twice with similar results.

Supplementary figure 9.

Glycyrrhizin (16 mg/mouse) and BoxA (2mg/mouse) were given intraperitoneally and topically, respectively, 2h before a single application of croton oil. The skins were collected 12h after the last treatment for RNA analysis. Real-time PCR analysis for inflammatory cytokine gene expression in the skin of TLR2 KO mice is shown. Results are expressed as fold induction over acetone-treated skins in each group after normalization to L32 mRNA. Values represent means +/- standard deviation of the mean from at least five mice in each group. The experiment was repeated twice with similar results. *, $P<0.05$

Supplementary figure 10.

A) Data table showing the statistical significant correlation between MyD88 and TLR4. Tissue microarray samples were compared for TLR4 and MyD88 expression and the association between the two genes was evaluated by ANOVA, Student's T-test and bar plot graphs. B) Immunohistochemical images showing upregulation of MyD88 in ovary and prostate tumor samples (T= 30) compared to normal tissues (N=7).

Supplementary Figure 11.

Schematic representation of TLR4 dependent skin tumorigenesis. A) CO or TPA treatment induces tissue damage-associated release of HMGB1, which is independent of TLR4 expression. In the absence of TLR4 expression (left), HMGB1 is unable to induce the release of inflammatory mediators and the recruitment of inflammatory cells. In the presence of TLR4 expression (right), HMGB1 can bind to resident TLR4 proficient cells and induces an initial wave of inflammatory cytokine production. At later time points, HMGB1 is also responsible for the recruitment of TLR4 proficient inflammatory cells. These cells release S100A8 and S100A9 proteins that are strong mediators of inflammation. B) Flow chart of the supposed sequence of events in TLR4 mediated skin tumorigenesis in formation of papillomas and carcinomas.

Supplementary table 1. Primers sequence for Real-time PCR

Gene	Sense	Antisense
L32	5'- CTGGAATTGTACCGCAGCTT -3'	5'- TCCTGTGCACACCATTTTTC -3'
IL1beta	5'- CCAAGCCTTATCGGAAATGA -3'	5'- TCACTCTTCACCTGCTCCAC -3'
IL6	5'- CCTGCTGAAGACCACAFATG -3'	5'- AGCTCCCTCTTGTTGTGGAA -3'
IL10	5'- TCTGAGCCACTCACATCTGC -3'	5'- TCAGGGGAACTGCTAGTGCT -3'
IL12a	5'- AGAGCTCGCAGTAGGGAACAG -3'	5'- CATCACCATGGCGTATGTG -3'
IL12b	5'- ACTATGGGGTTGAGGCACTG -3'	5'- ATCTCTCGGGACTCCTTGATG -3'
IL17	5'- CAGGACGCGCAAACATGA -3'	5'- GCAACAGCATCAGAGACACAGAT -3'
IL23	5'- AAGCGAAACTGGCGGAAAC -3'	5'- TAACCGATGTTGGGCATCAG -3'
TNFalpha	5'-TCTTCTCATTCCTGCTTGTGG-3'	5'-CACTTGGTGGTTTGCTACGA-3'
Cox2	5'- CCACTTCAAGGGAGTCTGGA-3'	5'- AGTCATCTGCTACGGGAGGA-3'
MMP9	5'- TCACTTTCCCTTCACCTTCG-3'	5'- AACACACAGGGTTTGCCTTC-3'
S100A8	5'- TCACCATGCCCTCTACAAGA-3'	5'- GCATTGTCACTATTGATGTCCAA-3'
S100A9	5'- TCAGACAAATGGTGGAAGCA-3'	5'- GCTCAGCTGATTGTCCTGGT-3'
KC	5'- GCTGGGATTCACCTCAAGAA -3'	5'- TCTCCGTTACTTGGGGACAC -3'
MIP-2	5'- AATGCCTGAAGACCCTGCCAAG -3'	5'- CTCCTTTCCAGGTCAGTTAGCC -3'

A

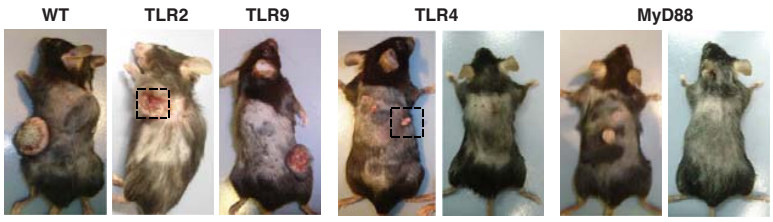

B

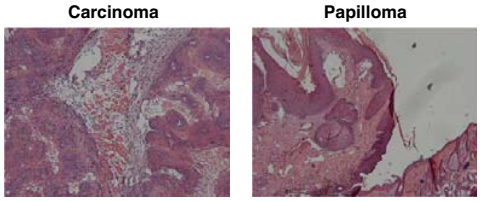

Mittal D, et al. Supplementary Figure 1

A

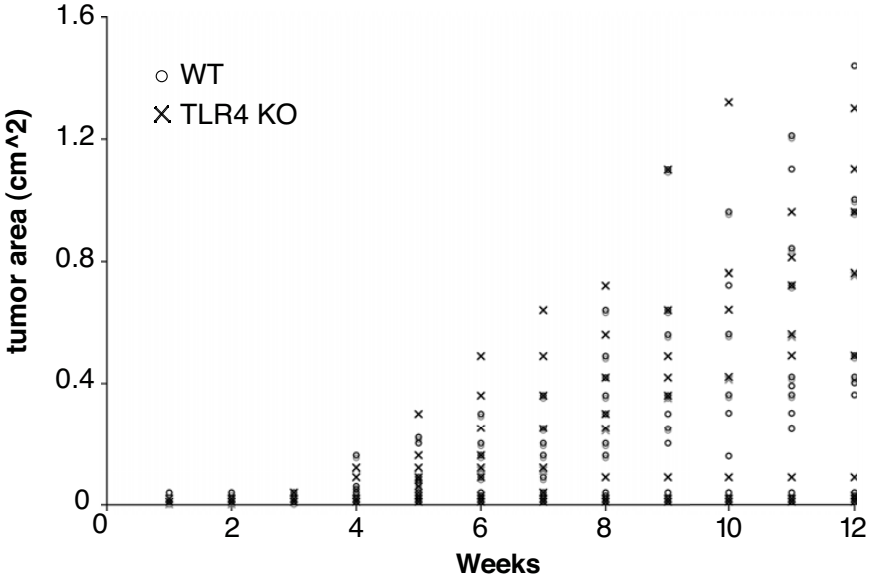

B

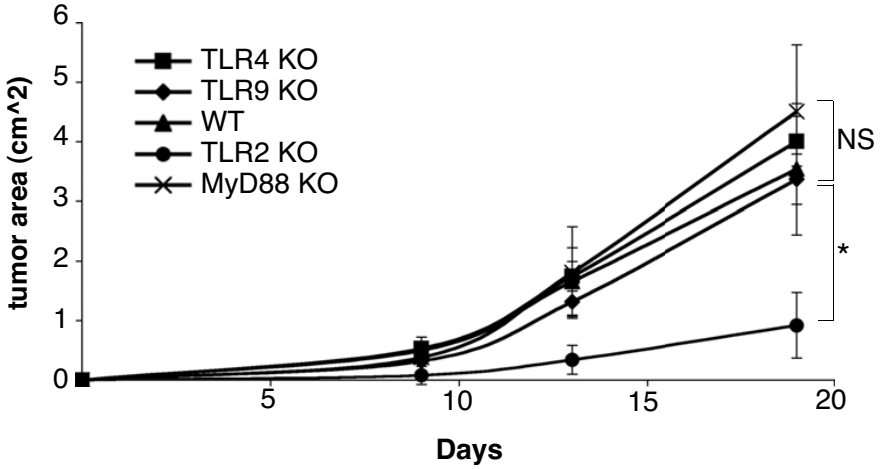

Mittal D, et al. Supplementary Figure 2

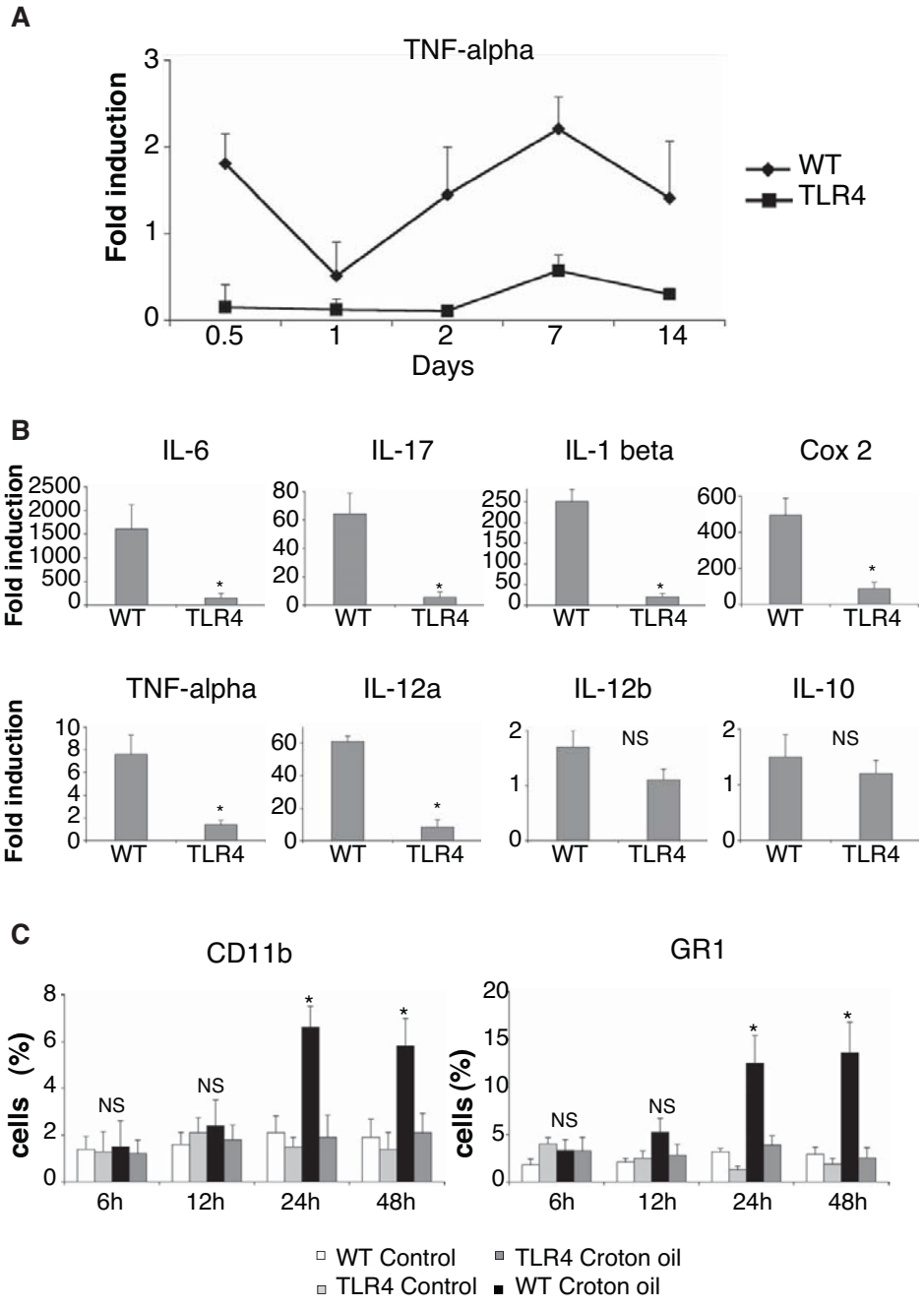

Mittal D, et al. Supplementary Figure 3

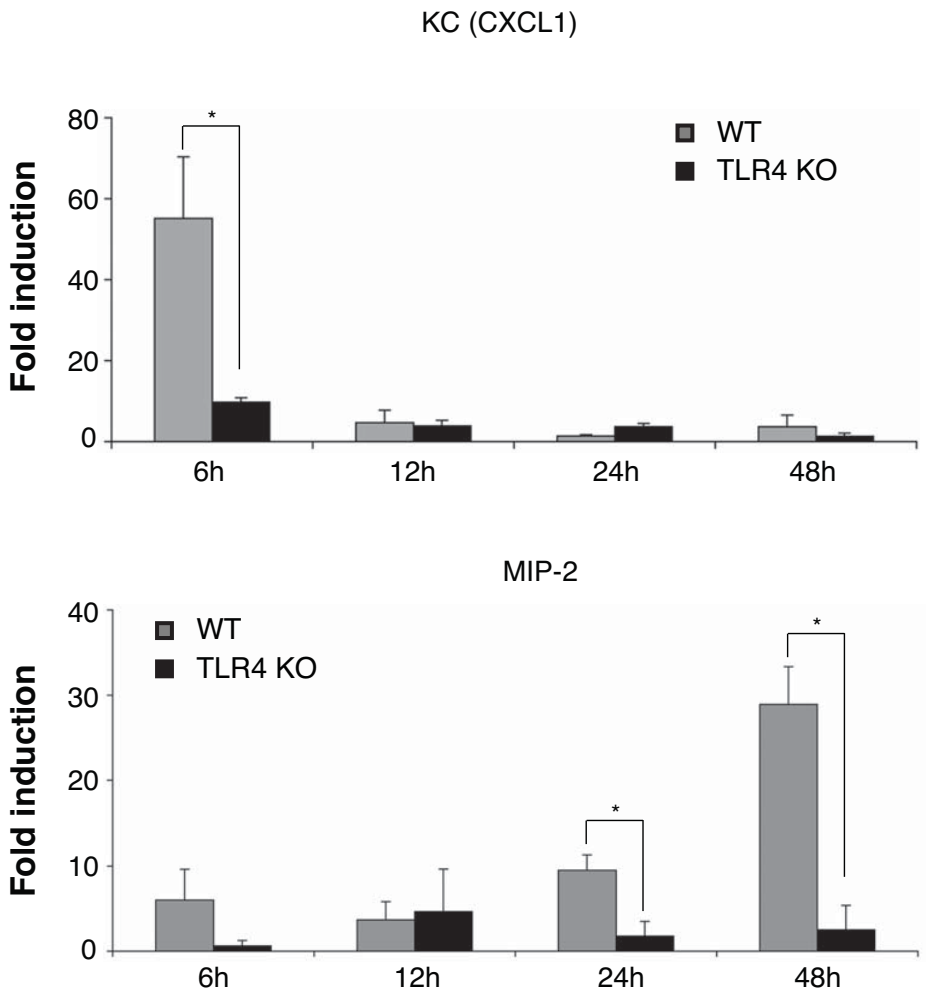

Mittal D, et al. Supplementary Figure 4

A

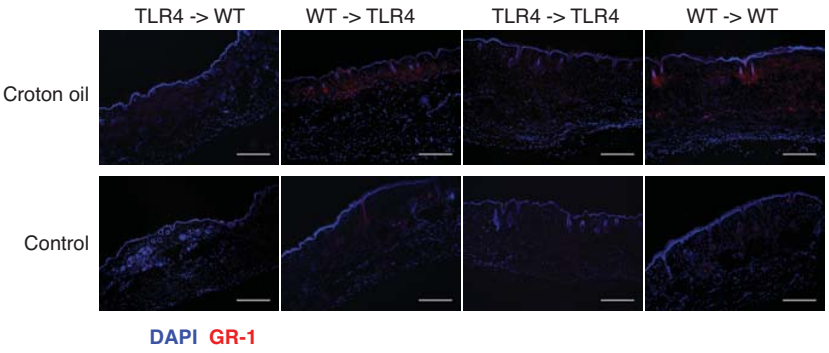

B

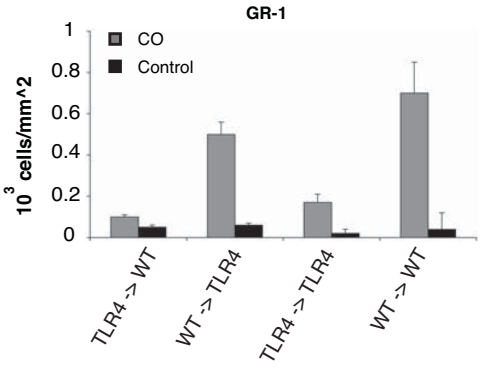

Mittal D, et al. Supplementary Figure 5

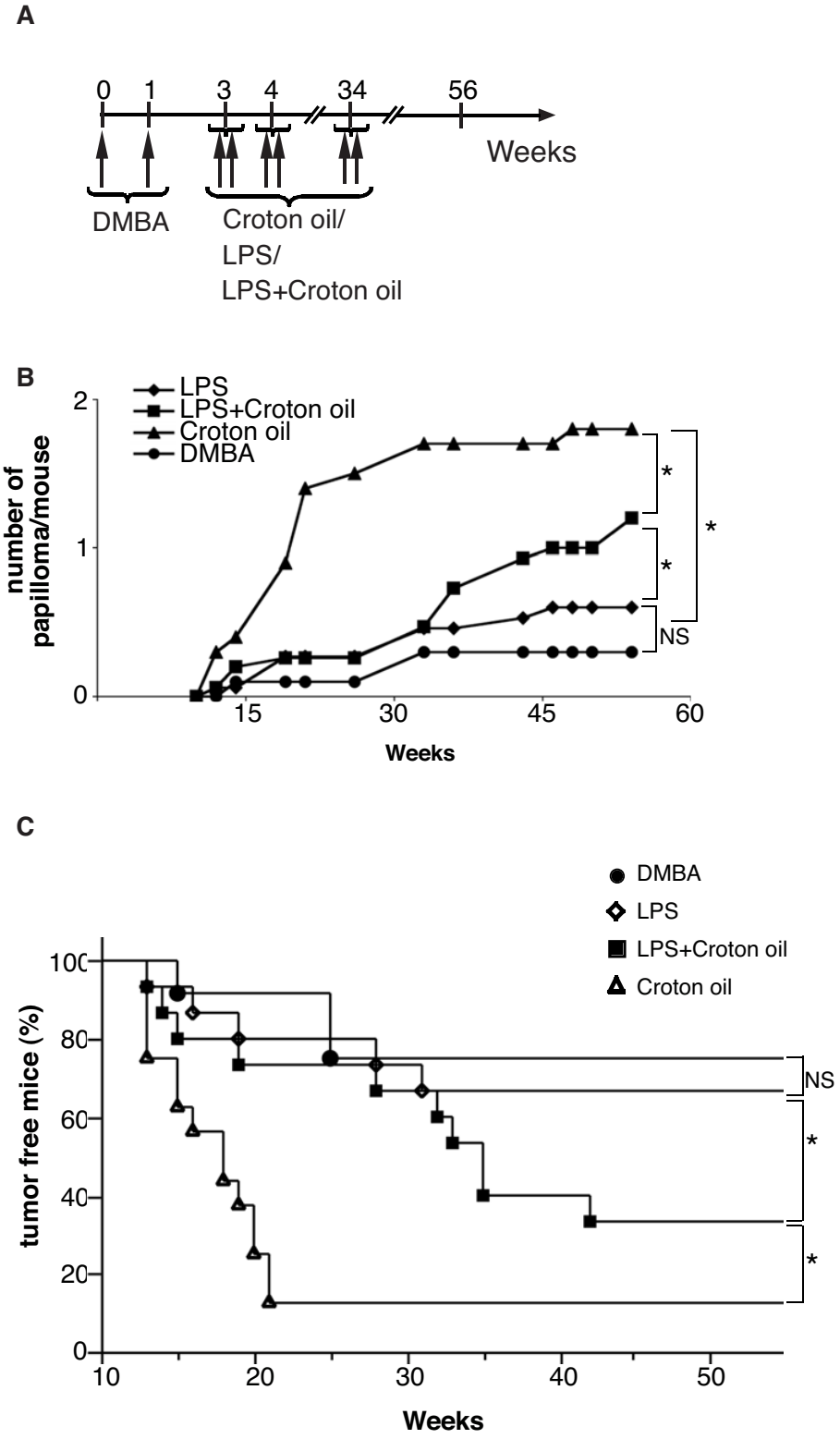

Mittal D, et al. Supplementary Figure 6

A

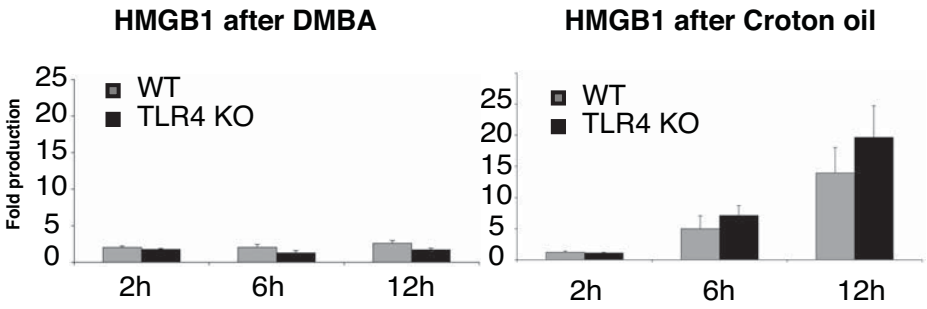

B

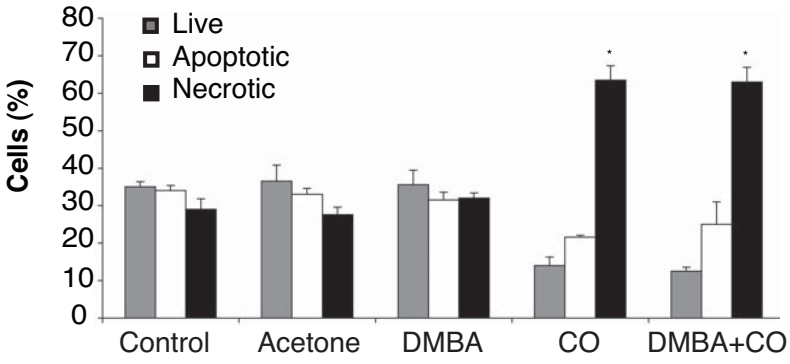

Mittal D, et al. Supplementary Figure 7

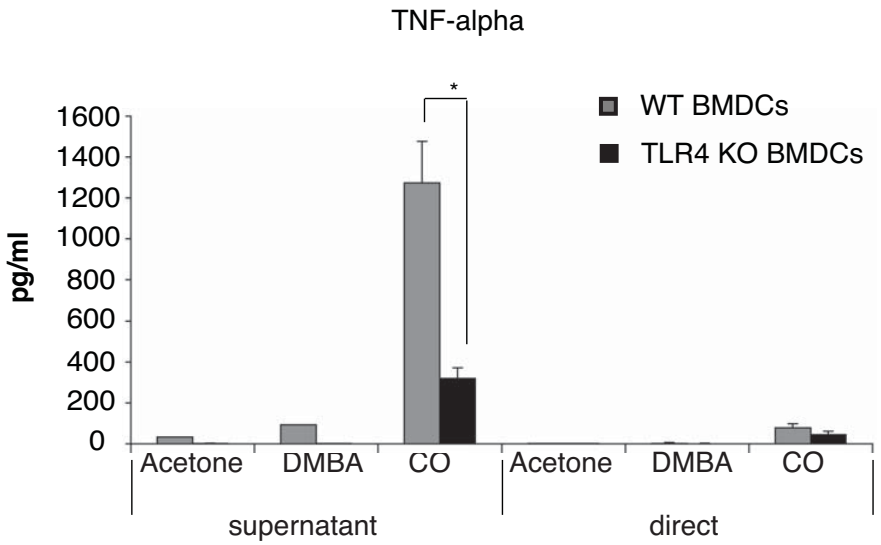

Mittal D, et al. Supplementary Figure 8

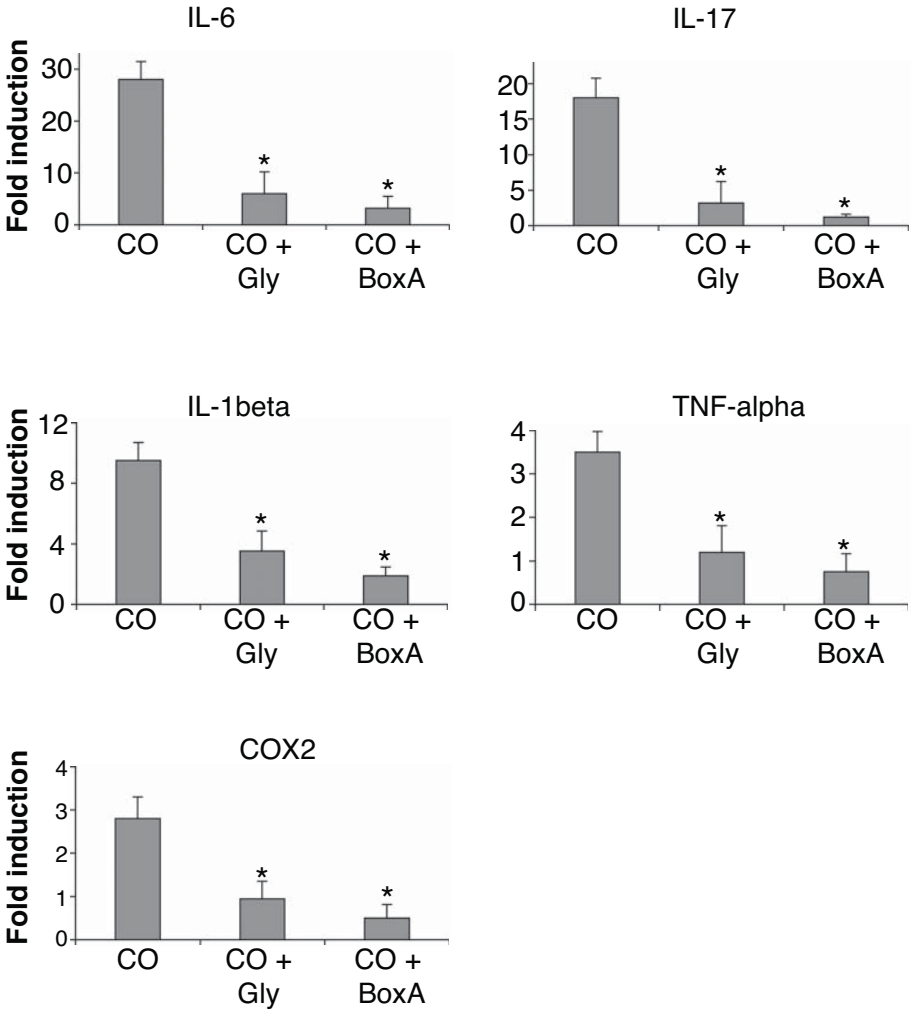

Mittal D, et al. Supplementary Figure 9

A

		TLR4 NEG (<1)	TLR4 POS (>=1)	
TLR4	*LOW (<=1)*	63	56 (47.1%)	
	HIGH (>1)	0	74 (100%)	**<0.001**
MYD88	*NEG (<1)*	52	25 (32.5%)	
	POS (>=1)	9	94 (91.3%)	**<0.001**
MYD88	*LOW (<=1)*	59	77 (56.6%)	
	HIGH (>1)	2	42 (95.5%)	**<0.001**

		MYD88 NEG (<1)	MYD88 POS (>=1)	
MYD88	*LOW (<=1)*	79	62 (44%)	
	HIGH (>1)	0	45 (100%)	**<0.001**
TLR4	*NEG (<1)*	52	9 (14.8%)	
	POS (>=1)	25	94 (79%)	**<0.001**
TLR4	*LOW (<=1)*	64	46 (41.8%)	
	HIGH (>1)	13	57 (81.4%)	**<0.001**

B

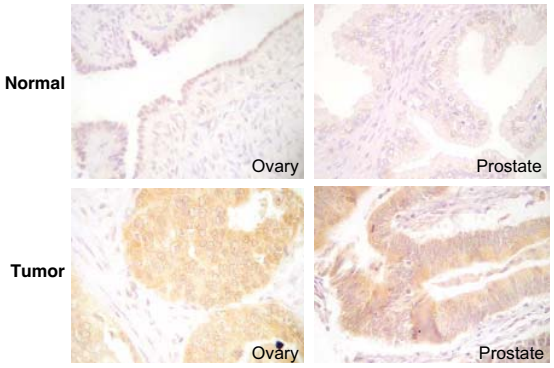

Mittal D, et al. Supplementary Figure 10

A

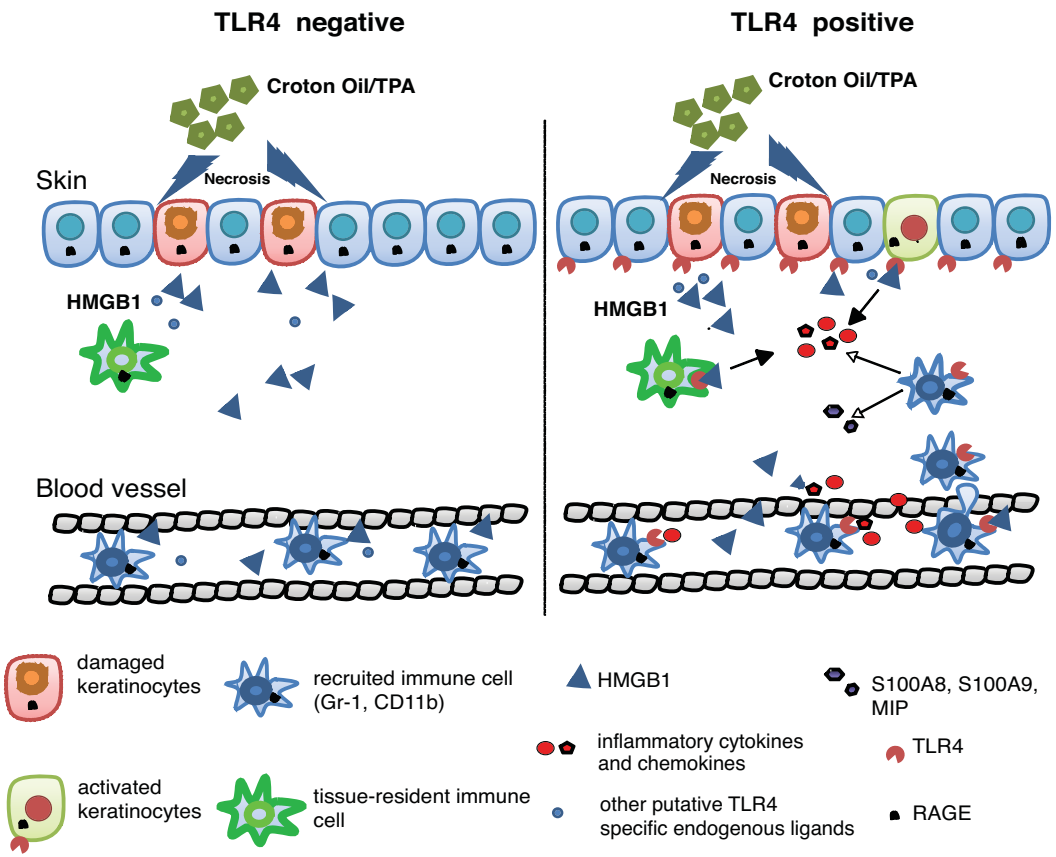

B

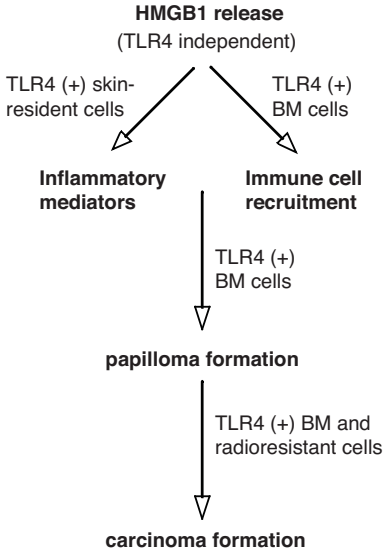

Mittal D, et al. Supplementary Figure 11